Journal of the Serbian Chemical Society
JSCS-info@shd.org.rs • www.shd.org.rs/JSCS
J. Serb. Chem. Soc. *91* (3) 271–289 (2026)
JSCS–5491
Original scientific paper
Published 26 February, 2026

Inclusion of $H_3PW_{12}O_{40}$ in cyclodextrin as a catalyst for oleic acid esterification

FERIEL TOUMI[1], YASMINA IDRISSOU[2,4], TASSADIT MAZARI[1]*, NICOLAS KANIA[3], ANNE PONCHEL[3], ABDENOUR BOUMACHHOUR[5], NOUARA LAMRANI[1] and CHERIFA RABIA[2]

[1]*Laboratory of Applied Chemistry and chemical engineering (LCAGC), Faculty of chemistry, University of Mouloud Mammeri Tizi Ouzou (UMMTO),Tizi Ouzou, Algeria,* [2]*Laboratory of Natural Gas Chemistry (LCGN), Faculty of Chemistry (USTHB), BP 32, 16111, Algiers, Algeria,* [3]*Jean Perrin Faculty of Sciences, University of Artois, UCCS-UMR CNRS 8181, Lens, France,* [4]*Ecole Normale Supérieure Kouba (ENS), Alger, Algeria and* [5]*Centre de Recherche Scientifique et Technique en Analyses Physico–Chimiques, Bou Ismail, Algeria*

(Received 27 August, revised 14 October, accepted 6 December 2025)

Abstract: This study focuses on the use of cyclodextrins (*β*-CD and HP-*β*-CD) as host materials to immobilize 20 wt. % tungstophosphoric acid, $H_3PW_{12}O_{40}$ (HPW), and their application as catalysts for the esterification of oleic acid, a fatty acid commonly found in many vegetable oils and frequently used as a biodiesel feedstock, into methyl oleate using methanol, the most commonly preferred alcohol for this reaction. The catalytic performances of these hybrid materials were compared with those of HPW incorporated into polyacrylamide hydrogel (20 wt. % HPW/PAAm) and HPW supported on silica (20 wt. % HPW/SiO_2), a conventional inorganic support. All materials were characterized by various techniques. For all supports, the Keggin structure of $H_3PW_{12}O_{40}$ was retained after immobilization, as confirmed by FT-IR and Raman spectroscopies. XRD and SEM analyses suggested the formation of inclusion complexes in the HPW/*β*-CD and HPW/HP-*β*-CD systems, as well as the successful incorporation of HPW into the PAAm matrix. In the esterification reaction carried out at 60 °C for 3 h, bulk HPW, HPW/PAAm and HPW/*β*-CD exhibited high catalytic activity, achieving methyl oleate yields of 97, 94 and 69 %, respectively, significantly higher than that obtained with the silica-supported catalyst (41 %).

Keywords: tungstophosphoric acid; polymer; cyclodextrin; esterification; methanol; methyl oleate.

* Corresponding author. E-mail: tassadit.mazari@ummto.dz
https://doi.org/10.2298/JSC250827095T

INTRODUCTION

The transition from fossil fuels to renewable energy sources has become a necessity if current environmental challenges are to be met. Among the viable alternatives, biodiesel has emerged as a promising candidate, alongside wind, solar, hydrothermal and photovoltaic energy. Biodiesel is not only non-toxic and biodegradable, but it also has similar physicochemical properties to those of conventional diesel fuel, with the advantage of reducing emissions of hazardous substances, thereby minimizing health risks.[1] Biodiesel, composed of fatty acid methyl esters, is produced by homogeneous or heterogeneous catalytic processes, involving the esterification or transesterification of renewable feedstocks such as vegetable oils and animal fats.

In the heterogeneous phase, various catalysts have been investigated for this purpose, including strontium-zinc bifunctional oxides[1] basic or acidic oxides,[2] *β*-zeolite-supported sulphated metal oxide[3] and silica supported tungsten oxide.[4] The methanolysis of oils using catalysts such as SiO_2/Al_2O_3 incorporated in BEA zeolite frameworks with alkaline earth oxides (MgO, CaO, SrO) has also been studied.[5]

In the homogeneous phase, alkaline catalysts such as sodium or potassium hydroxides, carbonates and alkoxides,[2,5] mineral acids (*e.g.*, phosphoric, sulfuric)[4] and heteropolyacids (HPAs[6,7] were found to be effective for fatty acids transesterification. However, although base-catalysed transesterification is generally more cost-effective than acid catalysis, it is still very sensitive to the presence of water and free fatty acids, and is also subject to undesirable side reactions such as hydrolysis and saponification,[8] which make it difficult to recover the desired product.

In acid catalysis, Keggin-type tungstophosphoric acid $H_3PW_{12}O_{40}$ (HPW), is particularly preferred due to its high Brønsted acidity and lower toxicity compared with conventional mineral acids. However, its high solubility in polar media complicates catalyst recovery and raises concerns about equipment corrosion and environmental impact, similar to those encountered with mineral acids.[9] To address these limitations, HPW has been immobilized on various solid supports, including zirconia,[10] alumina,[11]mesoporous silica[7] and activated carbon.[12] In oleic acid esterification in the presence of 30 wt. % HPW supported on biomass-derived activated carbon[12] and 20 wt. % HPW on KIT-6 mesoporous silica, a maximum conversion of 86 % was obtained. However, leaching is frequently observed with these conventional supports, which limits the long-term efficiency and reusability of the catalytic systems. The present study aims to reduce this drawback by incurporating HPW into polymeric matrices such as polyacrylamide (PAAm) hydrogels and cyclodextrins (CD).

Hydrogels are cross-linked, three-dimensional, superabsorbent polymer networks capable of retaining large volumes of water without dissolving.[13] Their

functional groups, including carboxylic, amide, amino, sulphonic acid and hydroxyl groups, provide active sites for molecular interactions.[14,15] Due to their high absorbency and interactive surface chemistry, hydrogels have been widely employed in biomedicine, biotechnology and catalysis. For example, Dharmapriya *et al.*[16] have demonstrated the efficiency of hybrid systems composed of hydrogels and catalytic species in the conversion of carbohydrates to 5-hydroxymethylfurfural. In order to improve the efficiency of hydrogels in acid reactions, several studies have suggested incorporating $H_3PW_{12}O_{40}$ (HPW), a heteropolyacid stronger than $H_3PW_{12}O_{40}$, into the polymer matrix. Thus, catalytic membranes constituted of HPW embedded in PVA polyvinyl alcohol (HPW@PVA), tested in glycerol acetalization with acetone, showed high conversion (95 %) and high selectivity and remained effective after ten reuse cycles without performance loss.[17] HPW encapsulated inside microporous polymeric nanospheres (H-MPNs) using a hyper-crosslinked PLA-b-PS polymer exhibits excellent catalytic activity and stability thanks to its hollow and permeable structure.[18] A series of composite materials (PLMTPA) synthesized by incorporating HPW into a polyacrylamide matrix at different ratios proved to be effective, recyclable and non-corrosive for the synthesis of 2-benzazepines under mild conditions and reusable over six cycles without loss of activity.[19] The HPW/polymer hydrogel system synthesized from a triethylene glycol monomer and a cross-linking agent, trapping heteropolyacid in the network through hydrogen bonds, effectively catalyses the hydrolysis of ethyl esters in an aqueous medium. It has been shown that HPW does not leach in water, allowing it to be used as a stable heterogeneous catalyst.[20]

Cyclodextrins (CDs), in particular *β*-CD and its derivatives, have attracted attention in pharmaceutical studies due to their ability to form host-guest inclusion complexes.[21] *β*-CD, composed of D-glucose units, has a hydrophobic internal cavity and a hydrophilic external surface, allowing it to encapsulate a variety of guest molecules. Its low water solubility, unique truncated cone shape, cost-effectiveness and ease of functionalization make it highly suitable for catalytic applications.[22–25] In addition to its pharmaceutical interest, *β*-CD has shown catalytic potential in various organic transformations.[26] For example, Wu *et al.* synthesized a hybrid complex $[La(H_2O)_9]\{[PM_{O_{12}}O_{40}]\subset[\beta\text{-CD}]_2\}$ (CD-POM-2), highlighting its catalytic, photocatalytic and biomedical utility.[27] Polyoxometalates (POMs) adsorbed in γ-cyclodextrin-based polymers (PVW_{11}@CD–EPI) through the chaotropic effect have been shown to form supramolecular hybrid materials exhibiting rapid and efficient adsorption behaviour as well as excellent catalytic performance. In the oxidation of benzyl alcohol, these hybrids achieved high conversion, selectivity and recyclability under mild reaction conditions.[28] Computational investigations based on density functional theory (DFT) and molecular dynamics simulations have revealed that POMs, such as $H_3PW_{12}O_{40}$ (HPW), can spontaneously penetrate the hydrophobic cavity of *γ*-cyclodextrin (*γ*-CD) to form stable host–

–guest complexes. This encapsulation significantly influences the electronic properties, reactivity and electron transfer behaviour of POMs, while the nanoconfinement effect contributes to the spatial isolation and stabilisation of the catalytic species.[29] In addition to Keggin-type POMs, the immobilization of Wells–Dawson-type POMs within cyclodextrin-based nanosponges (WD@CDNS) has also been reported to yield robust and durable catalytic systems. When applied to the Knoevenagel condensation reaction in aqueous media, the WD@CDNS catalyst demonstrated enhanced reusability and excellent structural integrity, confirming its potential for sustainable heterogeneous catalysis.[28] To our knowledge, the HPW/cyclodextrin system has not been tested in esterification or transesterification reactions.

In previous work, a 20 wt. % HPW/PAA catalyst system was tested for the esterification of oleic acid, a fatty acid commonly found in vegetable oils and frequently used as a biodiesel precursor. Methanol was chosen because of its low cost, small molecular size and wide availability.[30–32] Under an oleic acid:methanol:catalyst mole ratio of 1:29:0.025, a high conversion of 95 % was obtained with a reaction temperature and time of 60 °C and 3 h, respectively.[31] In the present study, the quantities of alcohol and catalyst were significantly reduced, and the oleic acid:methanol:catalyst molar ratio was adjusted to 1:9:0.008. Under these conditions, the catalytic performance of 20 wt. % HPW/PAAm was re-evaluated and compared with that of bulk HPW and three other catalytic systems: 20 wt. % HPW/SiO_2 (with silica as a conventional support), 20 wt. % HPW/β-CD and 20 wt. % HPW/HP-β-CD. The HP-β-CD derivative was obtained by substituting the hydroxyl groups of β-CD with hydroxypropyl functionalities.

EXPERIMENTAL

Material synthesis

All chemical reagents and solvents (from Biochem Chemopharma, Sigma–Aldrich and Riedel-De Haen) were used without further purification.

Tungstophosphoric acid ($H_3PW_{12}O_{40}$, HPW) was synthesized following a conventional method previously described in the literature.[33,34]

HPW (20 wt. %) was immobilized on silica (SiO_2), incorporated into a polyacrylamide hydrogel (PAAm), and included in β-cyclodextrin (β-CD) and hydroxypropyl-β-cyclodextrin (HP-β-CD). For the cyclodextrin-based systems, a stoichiometric ratio of five cyclodextrin units per Keggin unit was used.

Preparation of HPW/SiO_2

In a 100 mL two-neck flask, 1 g of HPW was dissolved in 15 mL of distilled water. The solution was heated in a sand bath (60–80 °C). Then, 4 g of silica (60–200 mesh) were gradually added under stirring. The suspension was refluxed at 110 °C for 5 h, followed by drying using a rotary evaporator. The resulting solid was placed in a vacuum oven at 50 °C for 6–7 h to remove residual moisture.[35]

Preparation of HPW/PAAm

Polyacrylamide hydrogel synthesis. In a three-neck round-bottom flask, 1 g of acrylamide monomer (C_3H_5NO) and 1×10^{-3} g of potassium persulfate ($K_2S_2O_8$) as an initiator were dissolved in ~3 mL of distilled water. After dissolution, 3×10^{-3} g of *N*,*N*′-methylenebisacrylamide ($C_7H_{10}N_2O_2$) was added as the crosslinker. The mixture was stirred at 250 rpm and purged with nitrogen (N_2) for 30 min to eliminate oxygen. The flask was then immersed in a water bath preheated to 60 °C and stirred for 20 min. A transparent PAAm formed at the bottom of the flask. The hydrogel was cut into small pieces, washed three times with distilled water to remove residual reagents and air-dried.[31]

HPW/PAAm preparation. dried PAAm was immersed in an aqueous solution of HPW (corresponding to 20 wt. % HPW). After complete absorption and air drying, the HPW-loaded hydrogel (HPW/PAAm) was recovered.

HPW/β-CD preparation

The HPW/*β*-CD system was prepared by physical impregnation, following a method similar to that used for HPW/SiO_2. In a 100 mL two-neck flask, 0.4 g of HPW was dissolved in 20 mL of water and heated in a sand bath maintained at 50–60 °C. Then, 1.6 g of *β*-cyclodextrin was gradually added. The suspension was refluxed at 80 °C for 5 h, followed by drying with a rotary evaporator.

HPW/HP-β-CD preparation

A mixture of 0.4 g of HPW and 1.6 g of HP-*β*-CD was stirred in ethanol for 24 h. The solvent was then evaporated using a rotary evaporator. The resulting white powder corresponded to the HPW/HP-*β*-CD system.

Characterization

The FT-IR spectra of the prepared catalysts were recorded on a Fourier transform spectrometer model IRAffinity-1S, Shimadzu, including an ATR module.

X-ray diffractograms of the catalytic materials were recorded on a Siemens D5000 powder diffractometer at room temperature over an angular range (2θ) of 0 to 70°, with CuKα radiation (λ = 1.5406 Å) at 45 kV and 40 mA. The step size and scanning speed were 0.026° and 2°/min, respectively.

The microstructural observations were performed using a Hitachi SU3800 scanning electron microscope (SEM) operated in backscattered electron (BSE) mode, under partial vacuum, at an accelerating voltage of 15 kV and a working distance (WD) of 10 mm. Energy-dispersive X-ray spectroscopy (EDS) analyses were conducted using a Bruker Quantax EDS system equipped with an XFlash detector.

Catalytic testing

The catalytic activities of bulk HPW and supported HPW systems (HPW/SiO_2, HPW/PAAm, HPW/*β*-CD, HPW/HP-*β*-CD) containing 20 wt. % HPW were evaluated for the esterification of oleic acid with methanol. Reactions were carried out at 60 °C under atmospheric pressure and reflux, with constant stirring at 300 rpm. The molar ratio of oleic acid:methanol:catalyst was 1:9:0.008. The detailed description of the sample preparation was presented in Table I. In a glass reactor, oleic acid and methanol were heated to 60 °C before adding the catalyst. After 3 h, the condenser was rinsed with minimal distilled water to recover the entire reaction mixture. The catalyst was separated by filtration (for supported catalysts), and the mixture was transferred to a separating funnel. Chloroform was added to facilitate phase separation. The organic (chloroformic) phase containing methyl oleate was collected, and the aqueous phase was

washed twice with chloroform to extract any remaining ester. The methyl oleate was recovered by evaporating the chloroform using a rotary evaporator.

TABLE I. Material weight and volumes of methanol and oleic acid used in sample preparation

Material	$W_{(catalyst)}$ / g	$V_{(oleic\ acid)}$ / ml	$V_{(methanol)}$ / ml
HPW	0.25	3	3.5
HPW/SiO_2	1.25	3	3.5
HPW/PAAm	0.0993	1.2	1.4
HPW/*β*-CD	0.625	1.5	1.75
HPW/Hp-*β*-CD	1.25	1.5	1.75
SiO_2	0.25	3	3.5
PAAm	0.0882	1.0584	1.2348
β-CD	0.25	3	3.5
HP-*β*-CD	0.25	3	3.5

The methyl oleate content was analyzed using gas chromatography (Agilent Technologies 7890A GC) equipped with a flame ionization detector (FID). The separation was performed on a capillary column (Carbowax, 30 m×0.25 mm) with nitrogen as the carrier gas (flow rate: 1 mL/min). The injector temperature was set at 260 °C. The oven temperature program was: 120––180 °C at 10 °C/min, followed by 180–260 °C at 7 °C/min, then held at 260 °C for final separation.

The yield of methyl oleate, the only product of the oleic acid esterification, considered in this study, was calculated from the following equation:[36]

$$R = 100\frac{C_{\text{methyl oleate}} \times F_d \times Q_{\text{methyl oleate}}}{m_{\text{oleic acid}}} \quad (1)$$

where $C_{\text{methyl oleate}}$: methyl oleate concentration (mg/μl), F_d: dilution factor, $Q_{\text{methyl oleate}}$: methyl oleate quantity (ml), $m_{\text{oleic acid}}$: oleic acid quantity (g).

RESULTS AND DISCUSSION

Characterizations

FT-IR and Raman spectroscopies. The FT-IR spectra of HPW, SiO_2 and HPW/SiO_2 are shown in Fig. 1a. The Keggin structure of HPW is identified by characteristic vibrational bands: asymmetric P–O_a stretching at 1072 cm^{-1}, asymmetric W=O_d at 964 cm^{-1}, asymmetric W–O_b–W at 887 cm^{-1} and W–Oc–W at 786 cm^{-1}.[37] The FT-IR spectrum of HPW/SiO_2 shows that the asymmetric stretching of Si–O in the 1200–1000 cm^{-1} region envelops the P–O_a vibration band (1072 cm^{-1}). Furthermore, the Si–O– band at 800 cm^{-1} merges with those corresponding to W–O_b–W (887 cm^{-1}) and W–Oc–W (786 cm^{-1}). IR spectroscopy does not allow the vibration bands of the heteropoly anion to be clearly distinguished from those of silica. It should be noted that the preparation method is impregnation, so the acid can only be fixed to the support after a strong interaction between the basic sites of the silica and the protons of the acid.

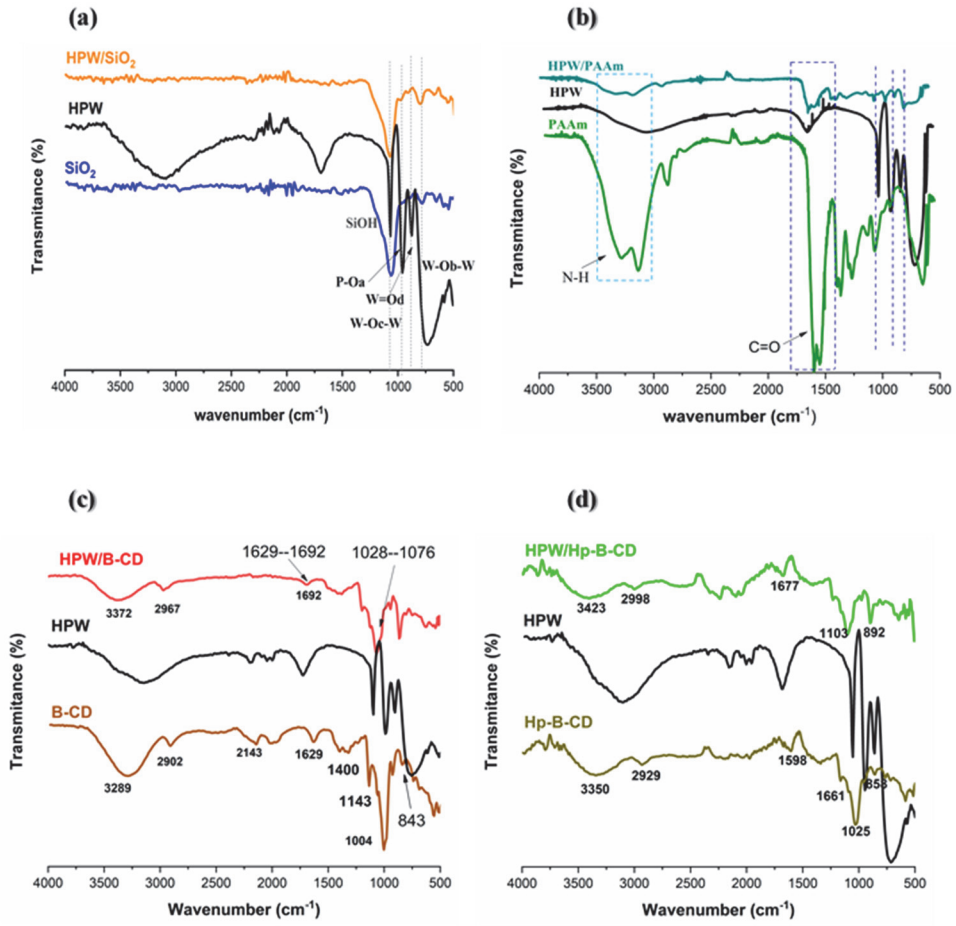

Fig. 1. FT-IR spectra of SiO_2, HPW and HPW/SiO_2 (a), PAAm, HPW and HPW/PAAm (b), β-CD, HPW and HPW/β-CD (c) and Hp-β-CD, HPW and HPW/Hp-β-CD (d).

Fig. 1b displays the FT-IR spectra of PAAm and HPW/PAAm. The spectrum of PAAm shows a strong band at 3334 cm^{-1}, characteristic of N–H stretching of primary amines, with two components at 3332 and 3189 cm^{-1} corresponding to asymmetric and symmetric N–H stretching, respectively. The intense band at 1640 cm^{-1} is assigned to C=O stretching, and the band at 1322 cm^{-1} to C–N bending vibrations of primary amides.[31] After incorporation of HPW into the hydrogel network, the FT-IR spectrum of HPW/PAAm shows the metal-oxygen vibrations of the heteropolyanion with reduced intensity, indicating that the structure of the Keggin unit is preserved.

The FT-IR spectra of β-CD (Fig. 1c) and HP-β-CD (Fig. 1d) are similar, displaying a broad band in the 3400–3200 cm^{-1} range, associated with O–H stretching

of primary alcohols in cyclodextrin, and a band near 2900 cm^{-1} corresponding to aliphatic C–H stretching. In the 1000–1150 cm^{-1} region, the observed bands are characteristic of C–O–C and C–C stretching.[24] Upon complexation with HPW, the FT-IR spectra of HPW/*β*-CD and HPW/HP-*β*-CD show the appearance of characteristic Keggin unit vibrational bands corresponding to the tungsten–oxygen and phosphorus–oxygen bonds, in the 1200–500 cm^{-1} region, with a slight shift towards high frequencies. Thus, the P–O_a vibration band shifts from 1072 to 1135 and 1063 cm^{-1}; the W=O_d band from 964 to 998 and 974 cm^{-1}; W–O_b–W from 887 to 917 and 888 cm^{-1}, and W–O_c–W from 786 to 822 and 797 cm^{-1} for HPW/*β*--CD and HPW/HP-*β*-CD, respectively. These shifts can be attributed to the formation of hydrogen bonds, as reported by some authors, thus indicating the complexation of HPW with cyclodextrin.[38,39]

The Raman spectra of both supported and unsupported $H_3PW_{12}O_{40}$ (Fig. 2) were also recorded. The spectrum of pure HPW exhibits typical metal–oxygen vibrations of the Keggin structure: symmetric and asymmetric W=O_d stretching at

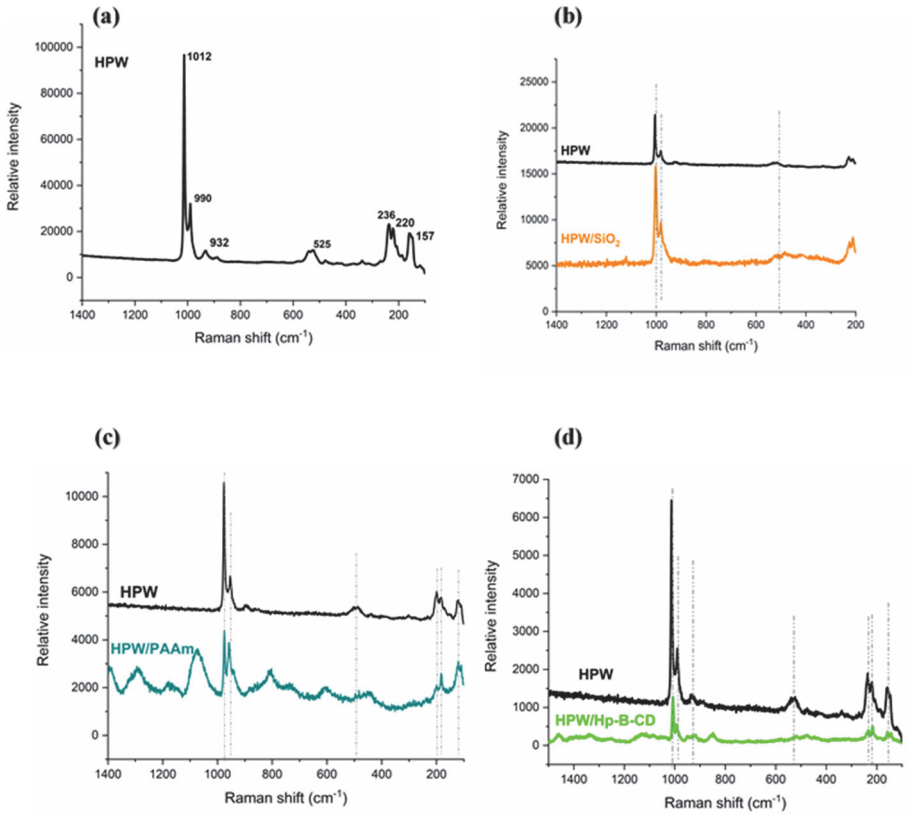

Fig. 2. Raman spectra of different catalysts, HPW (a), HPW and HPW/SiO_2 (b), HPW and HPW/PAAm (c) and Hp-*β*-CD, HPW and HPW/Hp-*β*-CD (d).

1012 and 990 cm^{-1}, asymmetric W–O_b–W at 932 and 525 cm^{-1}, and asymmetric W–O_c–W at 236 and 220 cm^{-1}.[37] In the support presence, the most intense vibration band corresponding to W=O_d shows a decrease in intensity, whatever the nature of the support, which is consistent with the FT-IR results, suggesting a strong interaction between the Keggin anion and the support, due to the high electron density of the tungsten-terminal oxygen bond.

The XRD patterns of HPW, SiO_2 and HPW/SiO_2 are presented in Fig. 3a. HPW shows sharp diffraction peaks in the 2θ range of 5.6–34.6°, characteristic of its triclinic phase (JCPDS Card No. 50-0655).[40,41] SiO_2 displays a broad peak between 15 and 23°, indicating its amorphous nature. The XRD pattern of HPW/ /SiO_2 shows weak peaks at 2θ around 9 and 20°, confirming the presence of HPW's triclinic structure. The low intensity of these peaks suggests a homogeneous dispersion of HPW (pore size: 84.3 Å) on the SiO_2 surface (250–74 μm).[7]

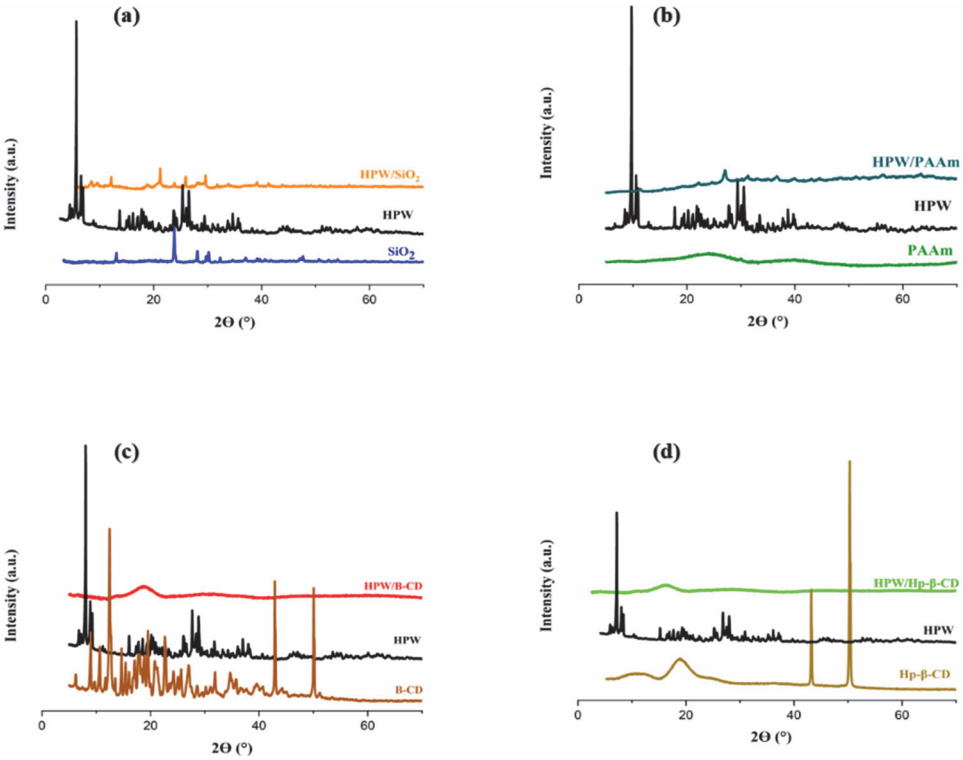

Fig. 3. X-ray diffraction patterns of SiO_2, HPW and HPW/SiO_2 (a), PAAm, HPW and HPW/PAAm (b), β-CD, HPW and HPW/β-CD (c) and Hp-β-CD, HPW and HPW/Hp-β-CD (d).

Fig. 3b shows the XRD patterns of the PAAm and HPW/PAAm. With PAAm alone, a broad peak extending between 2θ 17 and 32° was observed. After introduction of the heteropolyacid, no peaks characteristic of its tricilinic structure

were observed in the 2θ range between 10 and 20°, and only the peak located at 2θ 27° was observed with higher intensity. These results show that HPW is well inserted into the polymer cavities.

The XRD pattern of β-CD (Fig. 3c) displays multiple sharp lines between 2θ 0 and 50°, with dominant peaks at 10, 40 and 48°, confirming its crystalline nature.[42] In contrast, the XRD pattern of the HPW/β-CD complex shows the disappearance of all characteristic peaks of HPW and β-CD, replaced by a broad diffraction peak in the 10–20° 2θ range. This result suggests that β-CD, with its hydrophobic inner cavity and hydrophilic outer surface, can form inclusion complexes *via* host–guest interactions and hydrogen bonds with cyclodextrin cavities which can disrupt the β-CD structure.

Similarly, HP-β-CD exhibits a broad peak between 15 and 25°, along with sharper peaks at 41 and 50°, indicating the presence of small crystalline domains within an otherwise amorphous matrix.[43] After HPW incorporation, the XRD pattern of HPW/HP-β-CD resembles that of HPW/β-CD, with a broad peak between 2θ 10 and 20°, confirming the formation of similar inclusion complexes in both systems.

SEM

The SEM micrograph of HPW/SiO_2 (Fig. 4) reveals irregularly shaped blocks and rod-like structures, characteristic of the SiO_2 support. HPW is observed as white spherical nanoparticles, heterogeneously dispersed across the surface, forming a relatively uniform layer. These morphological features are consistent with the XRD analysis. Elemental mapping by EDX confirms the presence of silicon, tungsten and oxygen, supporting the successful immobilization of HPW on the silica surface.

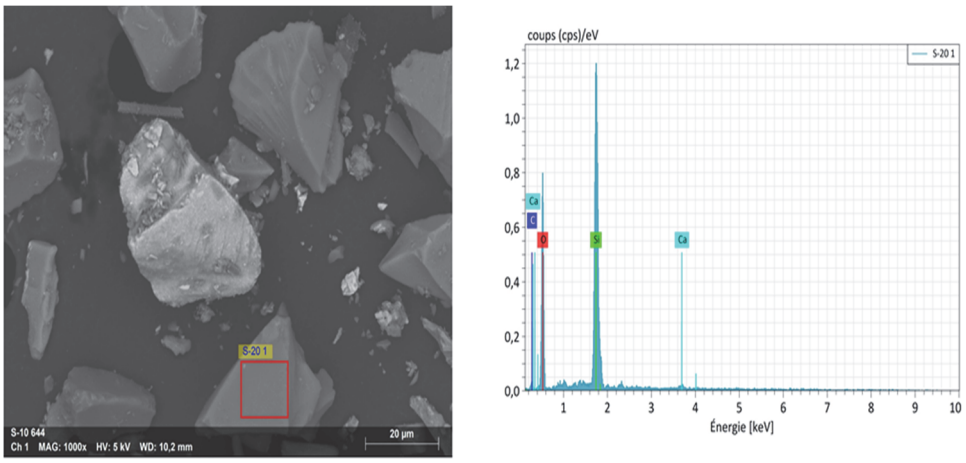

Fig. 4. SEM and elemental analysis (EDX) of HPW/SiO_2.

The SEM image of PAAm displays a smooth, dense surface with craters of varying diameters, Fig. 5. Upon HPW incorporation, the HPW/PAAm system exhibits a rougher surface morphology, with visible fissures and embedded HPW nanoparticles both at the surface and within the hydrogel matrix. These changes likely result from interactions between the HPW species and the functional groups of the polyacrylamide network. The encapsulation of HPW and the formation of cross-linking zones within the hydrogel are thus revealed by the morphological transformation.

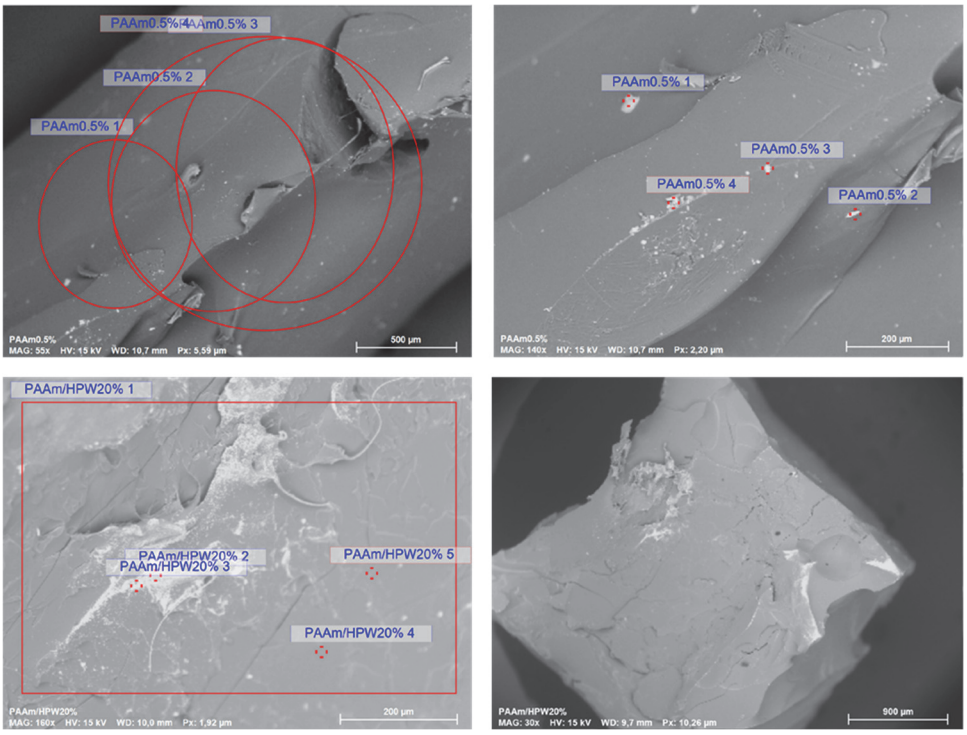

Fig. 5.SEM images of PAAm and HPW/PAAm.

At 20-μm magnification, the SEM images of HPW/*β*-CD and HPW/HP-*β*-CD materials reveal distinct morphologies. HPW/*β*-CD shows dark- and light-toned blocks with relatively flat surfaces, whereas HPW/HP-*β*-CD presents cauliflower--like aggregates and flat blocks surrounded by fine particles. These differences highlight morphological variations between the two systems. However, unlike in hydrogel-based systems, it remains difficult to confirm complexation or the inclusion of HPW within the cyclodextrin matrices based solely on SEM observations. EDX analysis confirmed the presence of tungsten in both systems, indicating the successful incorporation of HPW despite the morphological differences (Fig. 6).

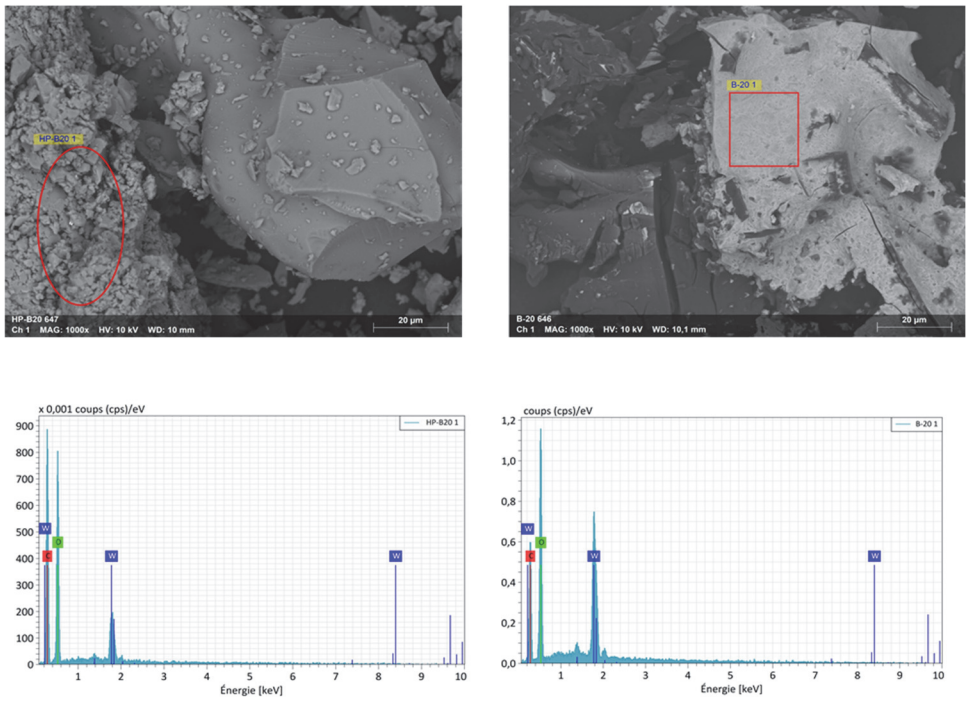

Fig. 6. SEM and elemental analysis (EDX) of HPW/*β*-CD and HPW/Hp-*β*-CD.

Catalytic results

The catalytic performances of bulk HPW and supported HPW systems, namely HPW/SiO_2, HPW/PAAm, HPW/*β*-CD and HPW/HP-*β*-CD, are summarized in Table II. The supports alone exhibited varying levels of catalytic activity, with methyl oleate yields of 40, 32, 9 and 8 % for *β*-CD, SiO_2, PAAm, and HP-*β*--CD, respectively. This intrinsic activity can be attributed to the basicity of the supports, originating from functional groups such as hydroxyl (OH) groups on silica and *β*-CD, and amino groups (NH_2) in polyacrylamide. It is well known that esterification and transesterification reactions are favoured by basic catalysts such as sodium or potassium methoxides, hydroxides and carbonates.[5] Bulk HPW showed the highest activity, achieving a methyl oleate yield of 97 %, attributable to its strong Brønsted acidity and high availability of acid sites in a homogeneous medium. However, upon immobilization, the catalytic performance of HPW decreased, with yields of 94, 69, 41 and 29 % observed for HPW/PAAm, HPW/*β*-CD, HPW/SiO_2 and HPW/HP-*β*-CD, respectively.

Among the supported catalysts, HPW/PAAm exhibited exceptional performance with a methyl oleate yield (94 %) nearly matching that of the bulk HPW (97 %). These results are similar to those obtained with an oleic acid:methanol:catalyst mole ratio of 1:29:0.025,[31] indicating that with less drastic conditions

(1:9:0.008) good results can be obtained. The efficiency of the HPW/PAAm catalyst is likely due to the three-dimensional cross-linked network of polyacrylamide, which allows for homogeneous dispersion of active sites throughout the matrix. The high catalytic activity can therefore be ascribed to the full availability of the protonic acid sites of HPW, effectively catalysing the esterification reaction.

TABLE II. Methyl oleate yields (%) as a function of catalyst type. Reaction temperature and time of 60 °C and 3 h, pressure:1 at, stirring: 300 rpm, oleic acid/methanol/catalyst mole ratio was 1/9/0.008

Catalytic system	Methyl oleate yield, %
HPW (bulk)	97
SiO_2	32
HPW/SiO_2	41
PAAm	9
HPW/PAAm	94
β-CD	40
HPW/*β*-CD	69
HP-*β*-CD	8
HPW/HP-*β*-CD	29

The HPW/*β*-CD system produced 69 % methyl oleate, which is significantly lower than the yield obtained with the HPW/PAAm system (94 %). This may be due to the hydrophobic nature of *β*-CD, which can restrict the accessibility of polar reagents such as methanol. The reduced catalytic activity of HPW/*β*-CD and HPW/SiO_2 is likely due to the strong hydrogen bonding interactions between HPW protons and hydroxyl groups on the supports, which reduce the availability of acidic sites for catalysis. Assuming a stoichiometric ratio of five *β*-CD units per Keggin unit in the HPW/*β*-CD system, it is likely that the hydrophobic cavities of *β*-CD develop a preferential affinity for the reactants, favouring the formation of microreactors composed of *β*-CD, oleic acid and methanol. In this configuration, HPW, being hydrophilic, acts peripherally to catalyse the surface reaction. This hypothesis is supported by scanning electron microscopy observations, which show that heteropolyacid molecules are surrounded by *β*-CD units.

The HPW/HP-*β*-CD catalyst only gave a yield of 29 %, lower than that of the *β*-CD (40 %) and SiO_2 (32 %) supports alone. This suggests not only a lack of basic sites but also a reduction in accessible acidic sites. The difference in performance between HPW/HP-*β*-CD and HPW/*β*-CD – despite their similar structures observed in XRD, can be attributed to steric hindrance caused by hydroxypropyl substituents in HP-*β*-CD, which likely obstruct reagent access to HPW active sites.

The catalytic efficiency obtained with a reaction temperature and time of 60 °C and 3 h and oleic acid:methanol:catalyst mole ratio of 1:9:0.008, across the systems follows the order: HPW (97 %) > HPW/PAAm (94 %) > HPW/*β*-CD (69 %) > HPW/SiO_2 (41 %) > HPW/HP-*β*-CD (29 %).

In the esterification of oleic acid, the HPW/PAAm catalytic system appears to be a more promising candidate than PW/UiO/CNTs–OH[44] and HPW/OMS–SO_3H[45] because it achieves a similar yield (93–95 %) but with better operating conditions (oleic acid/methanol/catalyst mole ratio of 1:9 *versus* 30:1 and 14.27:1, and a reaction temperature of 60 *vs.* 69 and 120 °C, respectively). In addition, the system can be reused several times without loss of catalytic activity. It should be noted that the HPW/*β*-CD system can also be considered attractive with a yield of 69 %.

Catalyst leaching was investigated by performing the oleic acid esterification reaction followed by FT-IR analysis of the reaction media (Fig. 7). After 1 h of methanolysis with HPW/PAAm or HPW/*β*-CD, no characteristic bands of the heteropolyacid were detected in the reaction mixture, confirming that HPW remained immobilized. This demonstrates the successful entrapment of HPW in the PAAm hydrogel network and its effective complexation within the *β*-CD structure.

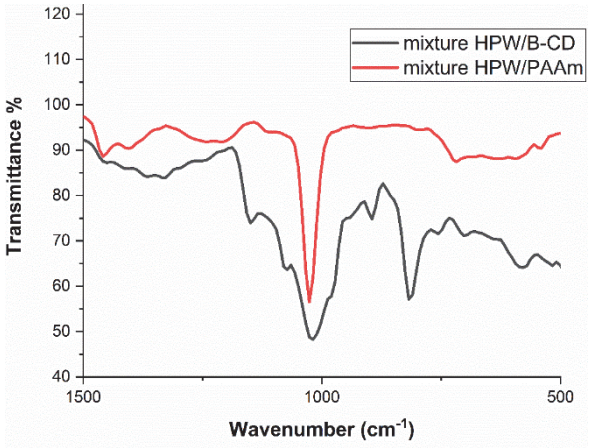

Fig. 7. FT-IR spectra of esterification reaction mixtures in the presence of HPW/PAAm and HPW/*β*-CD.

Stability tests were conducted over multiple cycles (3 h each) under identical reaction conditions (temperature: 60 °C; oleic acid/methanol/catalyst ratio: 1/9/0.008). For HPW/PAAm, the catalyst was separated, washed, dried, and reused. In the case of HPW/*β*-CD, the catalyst was kept at the flask bottom to minimize losses and then washed with ether and reused. Fig. 8 shows the yields of methyl oleate as a function of the number of cycles in the presence of the two catalyst systems, HPW/PAAM and HPW/*β*-CD. After six cycles, HPW/PAAm maintained a consistent methyl oleate yield of 94 %, indicating excellent recyclability and structural robustness. This contrasts with previously reported polymer-based catalysts such as hyper-crosslinked porous polymers, which showed a significant decrease in FAME yield from 99.9 to 42.5 % after just two cycles.[15] These results indicate

that, in this configuration, HPW is physically incorporated into the three-dimensional cross-linked network of the polyacrylamide hydrogel. The polar functional groups of the hydrogel (amide and carboxyl groups) provide interaction sites for the HPW molecules, allowing uniform dispersion in the polymer matrix. The resulting composite maintains the acid activity of HPW while preventing its leaching during catalysis, as observed in similar systems like HPW/SiO_2.[35] Conversely, the HPW/*β*-CD system exhibited structural degradation after only three cycles, in agreement with previous studies,[46,47] suggesting that CD-based materials may lack long-term stability under reaction conditions.

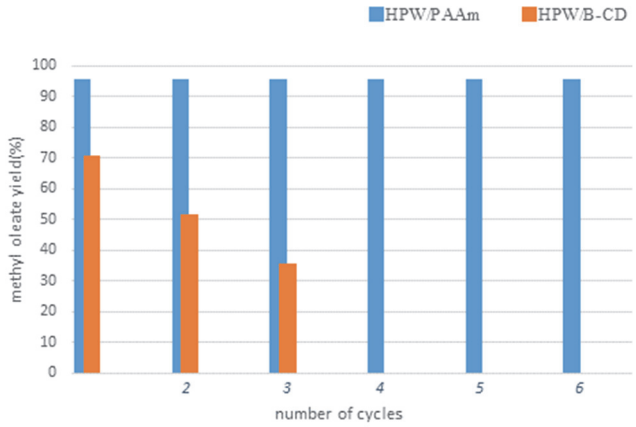

Fig. 8. Reusability of HPW/PAAm and HPW/*β*-CD in esterification reaction.

CONCLUSION

The novelty of this work lies in the use of organic materials as supports to immobilize a soluble polyoxometalate, tungstophosphoric acid ($H_3PW_{12}O_{40}$, HPW). The resulting catalytic systems were tested in the esterification of oleic acid to methyl oleate in the presence of methanol at 60 °C for 3 h. Polyacrylamide hydrogel (PAAm) and cyclodextrins (*β*-CD and HP-*β*-CD) were selected as organic supports, incorporating 20 wt.% HPW. For comparison, HPW supported on silica, a conventional inorganic material, was also evaluated.

Spectroscopic analyses (FT-IR and Raman) confirmed that the Keggin structure of HPW remained intact upon immobilization, regardless of the nature of the support. XRD and SEM results suggest the formation of host–guest inclusion complexes in the HPW/*β*-CD and HPW/HP-*β*-CD systems, and the successful incorporation of HPW into the PAAm hydrogel network.

Regarding their catalytic performance, HPW, HPW/PAAm and HPW/β-CD showed high activity in oleic acid esterification, yielding 97, 94 and 69 % of methyl oleate, respectively, which is significantly higher than the 42 % yield obtained with HPW/SiO_2.

No leaching of the heteropolyacid was detected after 1 h of reaction in the presence of HPW/PAAm or HPW/*β*-CD, as confirmed by FT-IR analysis of the reaction medium after catalyst separation. This highlights the effective retention of HPW within the PAAm network and its stable complexation with *β*-CD.

Catalyst stability tests over multiple cycles (3 h per cycle) revealed excellent reusability for HPW/PAAm, with a constant methyl oleate yield of 94 % even after six cycles. In contrast, degradation of the *β*-CD matrix was observed after only three cycles in the HPW/*β*-CD system.

These results highlight the potential of polyacrylamide hydrogels and cyclodextrins as efficient and environmentally friendly organic supports for the immobilization of a heteropolyacid, paving the way for cleaner and more sustainable catalytic processes.

These new materials have been designed to retain the high Brønsted acidity of HPW while improving its recyclability, dispersion and stability, in particular by minimizing leaching and improving compatibility with the reaction medium.

NOMENCLATURE

PAAm: Polyacrylamide hydrogel
β-CD: β-Cyclodextrin
Hp-*β*-CD: Hydroxypropyl-β-cyclodextrin
CDs: Cyclodextrins
SiO_2: Silica gel
HPW: Tungstophosphoricacid ($H_3PW_{12}O_{40}$)
HPAs: Heteropolyacids
FT-IR: Fourier transform infrared spectroscopy
Raman: Raman spectroscopy
SEM: Scanning electron microscopy
XRD: X-Ray diffraction
EDX: Energy-dispersive X-ray spectroscopy

ИЗВОД

ДОБИЈАЊЕ КАТАЛИЗАТОРА ЗА ЕСТЕРИФИКАЦИЈУ ОЛЕИНСКЕ КИСЕЛИНЕ УКЉУЧИВАЊЕМ $H_3PW_{12}O_{40}$ У ЦИКЛОДЕКСТРИН

FERIEL TOUMI[1], YASMINA IDRISSOU[2,4], TASSADIT MAZARI[1], NICOLAS KANIA[3], ANNE PONCHEL[3], ABDENOUR BOUMACHHOUR[5], NOUARA LAMRANI[1] и CHERIFA RABIA[2]

[1]Laboratory of Applied Chemistry and chemical engineering (LCAGC), Faculty of chemistry, University of Mouloud Mammeri Tizi Ouzou (UMMTO),Tizi Ouzou, Algeria,[2]Laboratory of Natural Gas Chemistry (LCGN), Faculty of Chemistry (USTHB), BP 32, 16111, Algiers, Algeria, [3]Jean Perrin Faculty of Sciences, University of Artois, UCCS - UMR CNRS 8181, Lens, France, [4]Ecole Normale Supérieure Kouba (ENS), Alger, Algeria и [5]Centre de Recherche Scientifique et Technique en Analyses Physico – Chimiques, Bou Ismail, Algeria

У овом раду је циклодекстрин (*β*-CD и HP-*β*-CD) коришћен као матрица за имобилизацију 20 мас. % волфрамфосфорне киселине, $H_3PW_{12}O_{40}$ (HPW) у циљу добијања

катализатора за естерификацију олеинске киселине у метил-олеат коришћењем метанола, који је најчешће коришћени алкохол за ову реакцију. Олеинска киселина је масна киселина која се налази у многим биљним уљима и често се користи као сировина за добијање биодизела. Каталитичке перформансе добијеног хибридног материјала су упоређене са материјалима који су добијени инкорпорирањем HPW у хидрогел полиакриламида (20 мас. % HPW/PAAm) и депоновањем HPW на SiO_2 као конвенционални неорганski носач (20 мас. % HPW/SiO_2). Сви материјали су окарактерисани различитим техникама. У свим случајевима, Кегин структура $H_3PW_{12}O_{40}$ је очувана након имобилизације, што је потврђено FT-IR и Раман спектроскопијом. XRD и SEM анализе су указале на формирање инклузионих комплекса у системима HPW/β-CD и HPW/HP-β-CD, као и успешно инкорпорирање HPW у PAAm матрицу. У реакцији естерификације на 60 °C за 3 h, HPW, HPW/PAAm и HPW/β-CD су показали велику каталитичку ефикасност, достигавши приносе метил-олеата од 97, 94 и 69 %, редом, много веће од приноса који је постигнут са 20 мас. % HPW/SiO_2 (41 %).

(Примљено 27. августа, ревидирано 14. октобра, прихваћено 23. децембра 2025)

REFERENCES

1. S. Liu, Z. Li, K. Han, Y. Wang, S. Niu, J. Liu, J. Zhu, Y. Zheng, *Chem. Eng. Proc. Proc. Intens.* **200** (2024) 109777 (https://doi.org/10.1016/j.cep.2024.109777)
2. G. B. Shimada, A. Cestari, *Renew. Energy* **156** (2020) 389 (https://doi.org/10.1016/j.renene.2020.04.095)
3. B. O. Yusuf, S. A. Oladepo, S. A. Ganiyu, *ACS Omega* **8** (2023) 23720 (https://doi.org/10.1021/acsomega.3c01892)
4. P. Prasertpong, J. Lipp, A. Dong, N. Tippayawong, J. R. Regalbuto, *Catalysts* **13** (2022) 38 (https://doi.org/10.3390/catal13010038)
5. K. A. V. Miyuranga, U. S. P. R. Arachchige, T. M. M. Marso, G. Samarakoon, *Catalysts* **13** (2023) 546 (https://doi.org/10.3390/catal13030546)
6. F. Esmi, S. Masoumi, A. K. Dalai, *Catalysts* **12** (2022) 658 (https://doi.org/10.3390/catal12060658)
7. Z. Wang, L. Liu, *Catal. Today* **376** (2021) 55 (https://doi.org/10.1016/j.cattod.2020.08.007)
8. Y. Patiño, L. Faba, E. Díaz, S. Ordóñez, *J. Environ. Manage.* **365** (2024) 121643 (https://doi.org/10.1016/j.jenvman.2024.121643)
9. M. Alotaibi, Md. A. Bakht, A. I. Alharthi, M. H. Geesi, I. Uddin, H. A. Albalwi, Y. Riadi, *Polycyc. Arom. Compd.* **42** (2022) 3089 (https://doi.org/10.1080/10406638.2020.1852588)
10. J. Alcañiz-Monge, B. E. Bakkali, G. Trautwein, S. Reinoso, *Appl. Catal., B* **224** (2018) 194 (https://doi.org/10.1016/j.apcatb.2017.10.066)
11. C. Leyvison Rafael V. da, C. E. R. Reis, R. de Lima, D. V. Cortez, H. F. de Castro, *RSC Adv.* **9** (2019) 23450 (https://doi.org/10.1039/C9RA04300D)
12. R. P. D. Almeida, R. C. Gomes Aciole, A. Infantes-Molina, E. Rodríguez-Castellón, J. G. Andrade Pacheco, I. D. C. Lopes Barros, *J. Clean. Prod.* **282** (2021) 124477 (https://doi.org/10.1016/j.jclepro.2020.124477)
13. R. Frenzel, D. Morales, G. Romanelli, G. Sathicq, M. Blanco, L. Pizzio, *J. Mol. Catal., A* **420** (2016) 124 (https://doi.org/10.1016/j.molcata.2016.01.026)

14. N. Kumar, R. Gusain, S. Pandey, S. S. Ray, *Adv. Mater. Interf.* **10** (2023) 2201375 (https://doi.org/10.1002/admi.202201375)
15. S. Señorans, E. Rangel-Rangel, E. M. Maya, L. Díaz, *React. Funct. Polym.* **202** (2024) 105964 (https://doi.org/10.1016/j.reactfunctpolym.2024.105964)
16. T. N. Dharmapriya, S.-Y. Wu, K.-L. Chang, P.-J. Huang, *J. Taiwan Inst. Chem. Eng.* **149** (2023) 104997 (https://doi.org/10.1016/j.jtice.2023.104997)
17. S. S. Balula, C. N. Dias, F. Mirante, *Available on SSRN* (2025): https://doi.org/10.2139/ssrn.5387449
18. Z. He, H. Wang, H. Yu, L. Zhang, C. Song, K. Huang, *React. Funct. Polymers* **169** (2021) 105063 (https://doi.org/10.1016/j.reactfunctpolym.2021.105063)
19. E. X. Aguilera Palacios, V. Palermo, A. G. Sathicq, L. R. Pizzio, G. P. Romanelli, *Catalysts* **12** (2022) 1155 (https://doi.org/10.3390/catal12101155)
20. J. Zhu, T. Gotoh, S. Nakai, N. Tsunoji, M. Sadakane, *Mater. Adv.* **2** (2021) 3556 (https://doi.org/10.1039/D1MA00278C)
21. G. Utzeri, P. M. C. Matias, D. Murtinho, A. J. M. Valente, *Front. Chem.* **10** (2022) 859406 (https://doi.org/10.3389/fchem.2022.859406)
22. M. Abbasi, *J. Chinese Chem. Soc*. **64** (2017) 896 (https://doi.org/10.1002/jccs.201600887)
23. D. Boczar, K. Michalska, *Pharmaceutics* **14** (2022) 1389 (https://doi.org/10.3390/pharmaceutics14071389)
24. B. Samannan, J. Selvam, J. Thavasikani, *Asian J. Chem.* **32** (2020) 297 (https://doi.org/10.14233/ajchem.2020.22321)
25. S. Teka, A. Jebnouni, A. A. O. Alrashidi, O. A. Alshammari, N. S. Jaballah, M. S. O. Alhar, M. Majdoub, *J. Mol. Struct.* **1308** (2024) 138044 (https://doi.org/10.1016/j.molstruc.2024.138044)
26. D. S. Dalal, D. R. Patil, Y. A. Tayade, *Chem. Rec.* **18** (2018) 1560 (https://doi.org/10.1002/tcr.201800016)
27. Y. Wu, R. Shi, Y.-L. Wu, J. M. Holcroft, Z. Liu, M. Frasconi, M. R. Wasielewski, H. Li, J. F. Stoddart, *J. Am. Chem. Soc.* **137** (2015) 4111 (https://doi.org/10.1021/ja511713c)
28. S. Aniba, N. Leclerc, C. Falaise, C. Roch-Marchal, S. Akriche, E. Cadot, M. Haouas, *Dalton Trans.* **54** (2025) 12534 (https://doi.org/10.1039/D5DT01317H)
29. M. Segado-Centellas, C. Falaise, N. Leclerc, G. Mpacko Priso, M. Haouas, E. Cadot, C. Bo, *Chem. Sci.* **15** (2024) 15849 (https://doi.org/10.1039/D4SC01949K)
30. F. A. N. Fernandes, *Catal. Res.* **2** (2022) 034 (https://doi.org/10.21926/cr.2204034)
31. Y. Idrissou, T. Mazari, C. Rabia, *J. Iranian Chem. Soc.* **19** (2022) 2553 (https://doi.org/10.1007/s13738-021-02474-8)
32. O. A. Mawlid, H. H. Abdelhady, M. G. Abd El-Moghny, A. Hamada, F. Abdelnaby, M. Kased, S. Al-Bajouri, R. A. Elbohy, M. S. El-Deab, *J. Clean. Prod.* **442** (2024) 140947 (https://doi.org/10.1016/j.jclepro.2024.140947)
33. H. S. Booth (Ed.), *Inorganic Syntheses, Volume I*, McGraw-Hill Book Company, New York, 1939
34. M. T. Pope, *Heteropoly and Isopoly Oxometalates*, Springer-Verlag, Berlin, 1983 (https://link.springer.com/book/9783662120064)
35. Y. Idrissou, T. Mazari, S. Benadji, M. Hamdi, C. Rabia, *React. Kin. Mech. Catal.* **119** (2016) 291 (https://doi.org/10.1007/s11144-016-1042-5)

36. C. Cannilla, G. Bonura, E. Rombi, F. Arena, F. Frusteri, *Appl. Catal., A* **382** (2010) 158 (https://doi.org/10.1016/j.apcata.2010.04.031)
37. C. Rocchiccioli-Deltcheff, M. Fournier, R. Franck, R. Thouvenot, *J. Mol. Struct.* **114** (1984) 49 (https://doi.org/10.1016/S0022-2860(84)87202-6)
38. H. Rachmawati, C. A. Edityaningrum, R. Mauludin, *AAPS PharmSciTech* **14** (2013) 1303 (https://doi.org/10.1208/s12249-013-0023-5)
39. A. Somer, J. R. Roik, M. A. Ribeiro, A. M. Urban, A. Schoeffel, V. M. Urban, P. V. Farago, L. V. D. Castro, F. Sato, C. Jacinto, E. Campesatto, M. S. A. Moreira, A. Novatski, *Mater. Chem. Phys.* **239** (2020) 122117 (https://doi.org/10.1016/j.matchemphys.2019.122117)
40. *Polyoxometalates: From Platonic Solids to Anti-Retroviral Activity*, M. T. Pope, A. Müller, Eds., Kluwer Academic Publishers, Dordrecht, 1994
41. P. Li, Z. Liu, Z. Xia, J. Yang, Optoelect. *Adv. Mater. Rapid Comm.* **17** (2023) 170 (https://oam-rc.inoe.ro/articles/phosphotungstic-acidsilicon-carbide-nanowire-heterostructure-photocatalyst-for-improving-photodegradation-of-rhodamine-b/)
42. D. Han, Z. Han, L. Liu, Y. Wang, S. Xin, H. Zhang, Z. Yu, *Int. J. Mol. Sci.* **21** (2020) 766 (https://doi.org/10.3390/ijms21030766)
43. P. Li, Q. Chen, B. Chen, Z. Liu, *Micro Nano Lett.* **15** (2020) 779 (https://doi.org/10.1049/mnl.2019.0734)
44. X. Xing, Q. Wu, L. Zhang, Q. Shu, *Catalysts* **15** (2025) 412 (https://doi.org/10.3390/catal15050412)
45. Z. Yu, X. Chen, Y. Zhang, H. Tu, P. Pan, S. Li, Y. Han, M. Piao, J. Hu, F. Shi, X. Yang, *Chem. Eng. J.* **430** (2022) 133059 (https://doi.org/10.1016/j.cej.2021.133059)
46. Y. A. Tayade, D. S. Dalal, *Catal. Lett.* **147** (2017) 1411 (https://doi.org/10.1007/s10562-017-2032-6)
47. R. S. Thombal, A. R. Jadhav, V. H. Jadhav, *RSC Adv.* **5** (2015) 12981 (https://doi.org/10.1039/C4RA16699J).